論文

T800/924C 탄소-에폭시 복합재판의 압축강도에 대한 두께 효과

이정환*, 공창덕**+, C. Soutis***

Thickness Effect on the Compressive Strength of T800/924C Carbon Fibre-Epoxy Laminates

J. Lee*, C. Kong**+ and C. Soutis***

ABSTRACT

In this study, the effect of laminate thickness on the compressive behaviour of composite materials is investigated through systematic experimental work using the stacking sequences, $[0_4]_{ns}$, $[45/0/-45/90]_{ns}$ and $[45_n/0_n/-45_n/90_n]_s$ (n=2 to 8). Parameters such as fibre volume fraction, void content, fibre waviness and interlaminar stresses, influencing compressive strength with increasing laminate thickness are also studied experimentally and theoretically. Furthermore the stacking sequence effects on failure strength of multidirectional laminates are examined. For this purpose, two different scaling techniques are used; (1) ply-level technique $[45_n/0_n/-45_n/90_n]_s$ and (2) sublaminate level technique $[45/0/-45/90]_{ns}$. An apparent thickness effect existes in the lay-up with blocked plies, i.e. unidirectional specimens ($[0_4]_{ns}$) and ply-level scaled multidirectional specimens ($[45_n/0_n/-45_n/90_n]_s$). Fibre waviness and void content are found to be main parameters contributing to the thickness effect on the compressive failure strength. However, the compressive strength of the sublaminate level scaled specimens ($[45/0/-45/90]_{ns}$) is almost unaffected regardless of the specimen thickness (since ply thickness remains constant). From the investigation of the stacking sequence effect, the strength values obtained from the sublaminate level scaled specimens are slightly higher than those obtained from the ply level scaled specimens. The reason for this effect is explained by the fibre waviness, void content, free edge effect and stress redistribution in blocked 0° plies and unblocked 0° plies. The measured failure strengths are compared with the predicted values.

초 록

본 연구에서 복합재의 압축 강도에 대한 두께 효과가 $[0_4]_{ns}$, $[45/0/-45/90]_{ns}$, $[45_n/0_n/-45_n/90_n]_s$ (n=2 to 8) 등의 적층 방법을 이용하여 체계적인 실험을 통해 조사되었다. 여기서 섬유 체적비, 기공률, 섬유 굴곡도, 층간 응력 등, 적층 두께 증가에 따른 압축 강도에 영향을 주는 파라미터 들이 실험과 이론적으로 연구되었다. 또한 엇교차 대칭 복합재판의 파괴강도에 대한 적층 순서 효과도 조사되었다. 이를 위해 2종류의 다른 스케일링 효과를 갖는 (1) 플라이-레벨 기법인 $[45_n/0_n/-45_n/90_n]_s$과 (2) 서브라미네이트-레벨 기법인 $[45_n/0_n/-45_n/90_n]_s$가 적용되었다. 일 방향 적층 시편 $[0_4]_{ns}$과 플라이-레벨인 $[45_n/0_n/-45_n/90_n]_s$에는 분명한 두께효과를 나타내었다. 그리고 섬유 굴곡도 와 기공률의 두께효과에 기여하는 주요 파라미터 들임이 확인 되었다. 그러나 서브라미네이트-레벨인, $[45/0/-45/90]_{ns}$의 압축강도는 시편 두께의 변화에도 불구하고 별 영향을 나타내지 않았으며, 서브라미네이트- 레벨 시편에서 구한 강도가 플라이-레벨 시편에서 구한 강도보다 약간 높았다. 이 같은 효과에 대한 이유는 섬유 굴곡도, 기공률, 자유단 효과 및 0°층과 비 0°층 사이의 응력 재 분포에 의한 영향인 것으로 보인다. 측정된 파괴강도는 예측 값과 비교되었다.

Key Words: 탄소섬유-에폭시 라미네이트(carbon fibre-epoxy laminate), 압축시험(compressive testing), 축척방법(scaling methods), 섬유 굴곡도(fibre waviness), 두께효과(thickness effect)

* The University of Sheffield, Aerospace Engineering, Graduate School, U.K.
**+ 조선대학교 항공 조선 공학부(항공 우주 전공), 교신저자(E-mail:cdgong@mail.chosun.ac.kr)
*** The University of Sheffield, Aerospace Engineering, U.K.

1. Introduction

As requirement for advanced composite materials in thick structural sections subjected to compressive loading has increased over recent years, understanding of the compressive behaviour of thick composite laminates becomes necessary. Few researchers have concentrated on studying the thickness effects on compressive strength due to the notorious difficulty of obtaining reliable test results. Existing test methods have not provided precise compressive properties to date due to the fact that all problems related with testing become more serious and complicated with thicker composites[1,2].

As the specimen gets thicker, a higher percentage of the load must be transmitted at the end, thus increasing the chances of premature failure such as end crushing[3]. For example, in considering composite cylinders subjected to external pressure, scale model testing has been conducted on un-stiffened cylinders nominally 203 mm in diameter with a wall thickness of 15 mm[4]. The test results of the thick cylinders have shown premature failure at stresses below the compressive strength measured in thin composite laminates. In addition Componeschil reported strength reductions of up to 35 % with increasing thickness (up to 12 mm) in unidirectional laminates through their experimental work. Although the above specimens failed prematurely, the test results revealed the tendency that the failure strength decreases with increasing thickness of composite laminates. The tendency was again identified by Daniel and Barzant's experimental results[2,3,5].

In this study, the effect of laminate thickness on the compressive behaviour of continuous fibre reinforced composites was investigated using the stacking sequences, $[0_4]_{ns}$, $[45/0/-45/90]_{ns}$ and $[45_n/0_n/-45_n/90_n]_s$ with and without an open hole. Parameters influencing the compressive strength with increasing laminate thickness were also identified experimentally and modelled theoretically. Finally the stacking sequence effects on failure strength caused by two different scaling techniques (ply level technique ($[45_n/0_n/-45_n/90_n]_s$) and sub-laminate level technique ($[45/0/-45/90]_{ns}$)) of the multidirectional laminates were examined and discussed in the following sections.

2. Experimental

2.1 Materials and Lay-ups

Table 1 Elastic Properties of the T800/924C system[6]

Property	E_{11} GPa	E_{22} GPa	G_{12} GPa	ν_{12}	σ_{11C} MPa	σ_{22C} MPa	$\tau_{12\#}$ MPa
Value	168	9.25	6.0	0.35	1615	250	105

(σ_{11C}=longitudinal compressive strength and σ_{22C}=transverse compressive strength)

The material used was T800/924C carbon fibre/epoxy system. The material was in the form of pre-impregnated tapes, which are 0.125 mm thick and commercially available by Hexcel Composites Ltd. The tapes were made of unidirectional Toray 800 carbon fibres, which are pre-impregnated with Hexcel 924C epoxy resin. The standard cure cycle recommended by manufacturers was used for the thin laminates less than 4mm thick. As the laminate thickness increases, the laminate has to dwell in an autoclave for a while to allow even heat distribution throughout the panel and to diminish possibility of exotherm (heat energy, which causes uncontrollable temperature rise within thick laminates). The thick laminate tested in this study initially dwell in the autoclave at 120°C using the following dwelling time: 30 minutes for 4 mm and 6 mm thick laminates and 45 minutes for 8 mm thick laminates. The in-plane stiffness and strength properties of the T800/924C unidirectional laminates are given in Table 1[6].

For laminate configuration, in this study two different approaches based on a quasi-isotropic stacking sequence were used, namely ply level scaling ($[45_n/0_n/-45_n/90_n]_s$) and sub-laminate level scaling ($[45/0/-45/90]_{ns}$) lay-ups made from the T800/924C system (n = number of plies 2, 3, 4, 6 and 8) for increasing thickness size effects. In addition, unidirectional laminates $[0_4]_{ns}$ (n = 2, 3, 4, and 8) were fabricated.

2.2 Specimen Geometry

Several specimens were cut from the panels of each thickness and glass fibre-epoxy reinforcement tabs were bonded giving gauge sections of 10 mm × 10 mm for the unidirectional specimens and 30 mm × 30 mm for the multidirectional. After tabbing, the specimens were machined to final tolerances by grinding all sides parallel and perpendicular to within 0.025 mm. For open hole specimens, a hole with a 3 mm hole diameter (diameter/width ratio, a/W = 0.1) was drilled at the centre of the specimens using a tungsten carbide bit to minimise fibre damage and delamination at the hole boundary. Penetrant

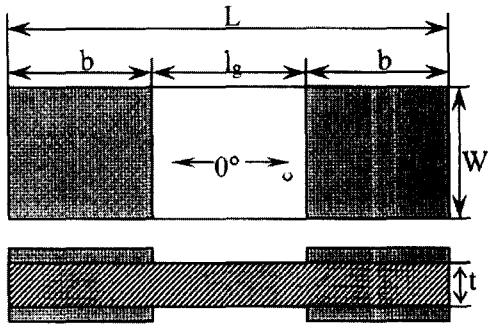

L = Total Specimen Length , lg = Gauge Length, b = Tab Length, W (Specimen Width) × lg (Gauge Length) = 10 mm × 10 mm for Unidirectional Specimen, W (Specimen Width) × lg (Gauge Length) = 30 mm × 30 mm for Multidirectional Specimen

Fig. 1 CFRP specimen dimensions.

enhanced X-ray radiography was used to inspect the quality of drilling.

The dimensions were based on those recommended by Airbus Industry Test method (AITM-1.008)[7]. The specimen thickness were changed from 2 mm to 8 mm. At least five specimens for each configuration were tested. A schematic representation of the specimen geometry is given in Fig. 1.

2.3 Compressive Testing

Static compressive tests were carried out on a screw-driven Zwick 1488 universal testing machine with a load capacity of 200 kN; a crosshead displacement rate of 1 mm/min was used. Load introduction to the specimen was mainly by end loading using an ICSTM fixture for unidirectional specimens and a modified ICSTM fixture for multidirectional specimens[8-9]. For 2 mm and 3 mm thick specimens, an anti-buckling device similar to that used by Soutis was employed to prevent column buckling. It contains a window at the device centre, allowing damage around the hole to occur but restraining the specimen from general bending. Frictional effects were minimised by lining the inner faces of the fixture with Teflon tape; the clearance between the anti-buckling device and the specimen face was less than 100 μm. The column length of the device is slightly shorter (~4 mm) than the specimen gauge length to allow for end-shortening of the specimen. Back-to-back strain gauges were attached on the specimens to monitor out-of-plane bending and of course record the failure strain[6].

Several of the tests were interrupted before final failure in order to examine damage growth. Examination was by dye-enhanced X-ray radiography. Zinc iodide solution has been

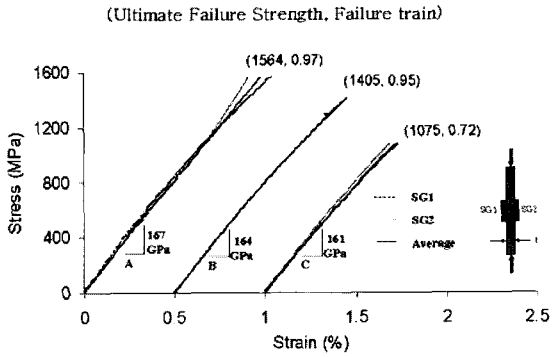

Fig. 2 Typical stress-strain curves of 2mm (A), 4mm (B) and 8mm (C) thick unidirectional specimens obtained from back-to-back strain gauges.

shown to be an effective penetrant for highlighting damage regions in composite laminates. The location and nature of damage in individual plies was obtained by using the de-ply technique and scanning electron microscopy (SEM). The de-ply method was performed by burning off most of the resin, while leaving just enough matrix to keep the fibres in position. The resin was burnt off in an appropriately ventilated furnace since the fumes that were released are toxic. For the multidirectional stacking sequence of T800/924C used in this study it was found that 30 minutes at a temperature of 400°C yielded optimum results. Once the resin had been burnt off the plies were carefully separated with a blade. These were then attached to a plate and then placed in the vacuum chamber of a JEOL JSM T220A scanning microscope, ready to be viewed. It is to be noted that since carbon is a good conductor there was no need to coat the specimens in conductive material once the resin had been removed.

3. Test Strength Results

3.1 Unidirectional Specimens

Representative stress-strain curves of 2 mm (A), 4 mm (B) and 8 mm (C) thick unidirectional specimens obtained from back-to-back strain gauges are shown in Fig. 2. Plots B for the 4 mm thick specimen and C for the 8 mm thick specimen are offset by 0.5 % and 1.0 % strain, respectively, so results can appear on the same graph.

The consistency of the two strain gauge readings up to failure in each curve indicates that bending due to misalignment has been successfully minimized. The percent difference of back-to-back strain gauges is 0.1 % for 2 mm,

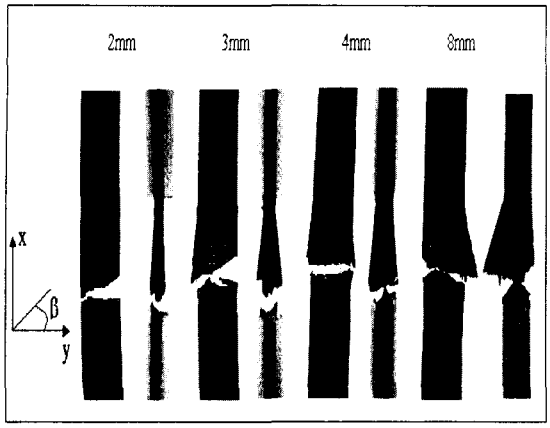

Fig. 3 Comparison of the post failure mode of the unidirectional specimens.

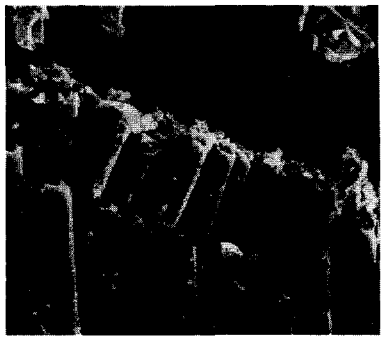

Fig. 4 SEM micrograph of fibre kinking in a unidirectional T800/924C laminate for 2 mm and 3 mm specimens.

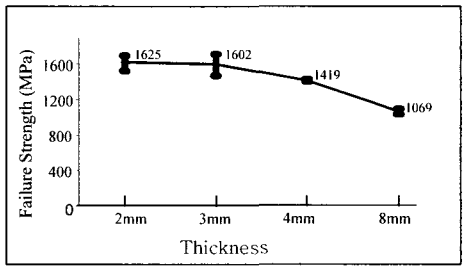

Fig. 5 Average compressive strength as a function of specimen thickness for T800/924C unidirectional laminates.

0.01 % for 4 mm and 0.05 % for 8 mm thick unidirectional specimens. These three curves show similar stress-strain behaviour, which is essentially linear up to an applied strain of approximately 0.5 %. Thereafter, the material behaves nonlinearly with a softening that increases with increasing strain. The compressive modulus was determined by averaging the initial slopes of the stress-strain curves from readings of back-to-back strain gauges at 0.25 % strain. The results indicate that the axial modulus for the T800/924C system measured at 0.25 % applied strain varies very little (less than 4 %) with specimen thickness.

Compressive failure of the unidirectional T800/924C carbon-epoxy composite for all thicknesses was instantaneous and catastrophic and was accompanied by an audible acoustic event but no cracking sound prior to the catastrophic failure. When failure occurred, the specimen parted into two pieces with fracture surfaces inclined at typical angles of between $\beta = 10°\sim30°$ (β: kink band inclination angle) from the horizontal axis as shown in Fig. 3.

After compression tests, some of the broken T300/924C specimens were selected and examined in the SEM. Fig. 4 depicts the microscopic feature of a typical fracture surface, in which the characteristic step features associated with microbuckling of the fibre forming a kind band are clearly evident as described in most publications. There is also little reason to doubt that failure in general is by microbuckling and kinking of fibres because the characteristic kink band angle is similar to the fracture surface angle of test piece fragments (see Fig. 3), though usually slightly larger. It is observed that the fibres break at two points, which create a band inclined at $\beta = \sim23°$ to the horizontal axis, where β is defined in Fig. 4. Kink band starts at the free edge or locations of stress concentration such as a pre-exiting material defect and load introduction, i.e. at the end of tabs where the specimen emerges from the band is propagated, keeping its direction

In most of the 4 mm and 8 mm thick specimens, failure occurred at the ends of the specimens at the load introduction point. The most predominant failure characteristic was that initiated at the top corner of the specimen and propagated down and across its width. Only one 4 mm thick and 8 mm thick specimen failed in the brooming failure mode. The measured failure strengths were, however, almost similar to or slightly less than those obtained with the more common brittle shear plane failure.

In addition, a couple of 4 mm and 8 mm thick specimens failed prematurely due to end crushing. This failure was not observed with the thinner specimens in the present study. The failure strength of the specimens, which failed by end crushing were lower compared to that of the specimens that failed in a brittle shear plane failure mode.

Fig. 5 presents the ultimate compressive failure strength as a function of specimen thickness with scatter bars. The curve shows a sharp decrease in compression strength with increasing

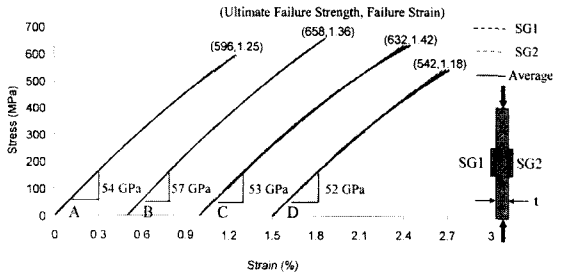

Fig. 6 Stress-strain curves of the multidirectional T800/924C laminates with sublaminate level scaling $[45/0/-45/90]_{ns}$ (4 mm thick specimen (A) and 6 mm thick specimen(B)) and ply level scaling $[45_n/0_n/-45_n/90_n]_s$ (4 mm thick specimen (c) and 6 mm tick specimen(D)).

thickness for the unidirectional specimens. The strength of the T800/924C unidirectional laminates dropped by approximately 2 % to 36 % in going from 2 mm to 8 mm thick specimens but near grip failures observed in the thicker specimens might contributed to the bigger strength reduction. The average failure strain of the 8 mm thick specimen was 0.72 % compared to 0.97 % for the 2 mm thick specimen.

3.2 Unnotched Multidirectional Specimens

Typical stress-strain curves are shown in Fig. 6 for the 4 mm (A) and 6 mm (B) thick specimens laminated with sublaminate level stacking sequence and the 4 mm (C) and 6 mm (D) thick specimens laminated with ply level stacking sequences. Lines of B,C and D are offset by 0.5 %, 1.0 % and 1.5 % strain, respectively, in Fig. 6.

The curves are linear up to a strain of approximately 0.5 % with softening behaviour to failure after that. The nonlinearity of the multidirectional specimens is higher than that of the 0°-unidirectional (see Fig. 2) due to matrix nonlinearity of the off-axis layers. The average failure strains of the multidirectional specimens (~1.2 % to 1.4 %) are also higher than that of the 0°-unidirectional (~1 %), suggesting that the mechanism of failure in the axial plies is affected by adjacent off-axis layers. The off-axis plies (±45°) provide lateral support to the 0° axial plies and delay the initiation of fibre microbuckling.

The measured elastic moduli at 0.25 % applied strain for the multidirectional T800/924C laminates tested are between 52-57 GPa, Fig. 6, compared to 61 GPa estimated by the laminate plate theory[25]. The difference may be due to manufacture imperfections and variability in fibre volume fraction, see later sections.

Test results for all thicknesses were valid and reproducible.

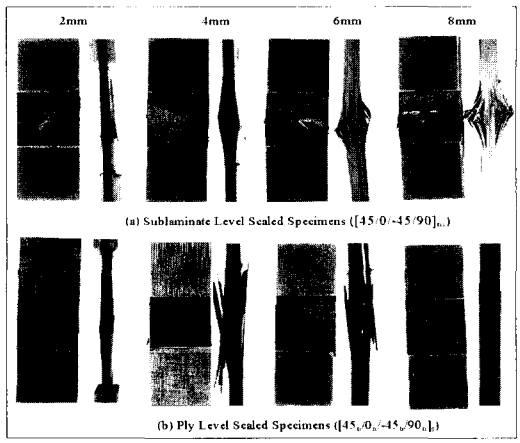

Fig. 7 Comparison of the overall failure mode of the multidirectional specimens.

All specimens regardless of specimen thickness failed within the gauge length. In the case of the multidirectional specimens using the sublaminate level scaling technique ($[45/0/-45/90]_{ns}$), failure was sudden and immediately prior to catastrophic fracture distinct cracking sounds were heard. However, compressive failure of the multidirectional specimens using the ply-level scaling technique ($[45_n/0_n/-45_n/90_n]_s$) was instantaneous and catastrophic and was accompanied by an audible acoustic event without cracking sound prior to the catastrophic failure. Figures 7 (a) and 7 (b) show the overall failure mode of the multidirectional specimens with the different thickness ranging from 2 mm to 8 mm. Post failure examination of the sublaminate level scaled specimens ($[+45/0/-45/90]_{ns}$) showed similar failure characteristics regardless of the specimen thickness. The failure involved a combination of fibre microbuckling in the 0° plies, delamination between 0° and ±45° plies, splitting parallel to the fibres at 0° and ±45° plies, and matrix cracking and crushing in the 90° plies. In addition, the failure seemed to occur in a crushing failure mode without a global buckling influence as shown at the side view in Fig. 7 (a). The ply level scaled specimens ($[45_n/0_n/-45_n/90_n]_s$) also showed the above failure characteristics in macro-scale, but in a more pronounced way. This includes clearer fibre splitting in the 0° and ±45° plies, more clear delamination between 0° and ±45° plies and more clear matrix cracking and crushing in the 90° plies as shown in Fig. 7 (b). The kink band angle, β, in the 0° plies is 10°-30° regardless of stacking sequence, which is similar to that observed in the 0°-unidirectional specimens.

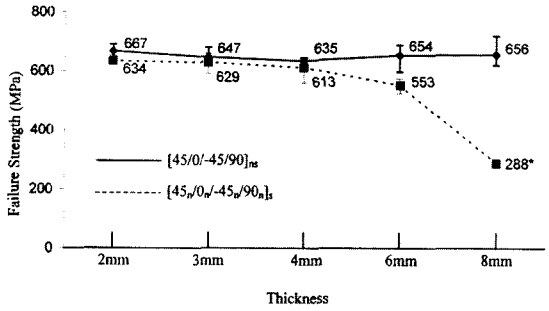

Fig. 8 Average compressive strength as a function of specimen thickness for T800/924C multidirectional laminates.

The failure mode and strength of the 8 mm thick specimen is quite different, compared with the failure mode of the thinner specimen (Fig. 7 (b)). Fig. 8 shows the ultimate compressive strength as a function of specimen thickness for the multidirectional specimens of both stacking sequences with scatter bars. The average failure strength values of the specimens using the sublaminate level scaling technique ($[45/0/-45/90]_{ns}$) are almost constant regardless of the specimen thickness, indicating that no significant thickness effect exists.

The strengths of the ply level scaled specimens ($[45_n/0_n/-45_n/90_n]_s$) are almost unaffected by thickness changes up to 4 mm, but drop by 10 % in going from 4 mm to 6 mm, showing a thickness effect. The 8 mm thick specimen's average strength is significantly lower than that of thinner specimens due to material brittleness (6 year old pre-preg) that caused premature failure. Finally when compared with the average failure strengths of both stacking sequences, the strength of the sublaminate level scaled specimens is slightly higher than that of the ones fabricated by using the ply level scaling technique

3.3 Fibre Volume Fraction

The influence of fibre volume fraction on the mechanical properties of composites under compressive load is reasonably well understood. When plates get thicker, the curing cycle should be changed accordingly. In this section, it is investigated whether the different curing cycles with increasing plate thickness have an influence on the fibre volume fraction of the plates.

The fibre and void content in T800/924C laminates were measured by using the resin acid digestion test suggested by BAE Systems. To achieve this four experimentally obtained parameters (specimen mass, fibre mass, specimen density, and

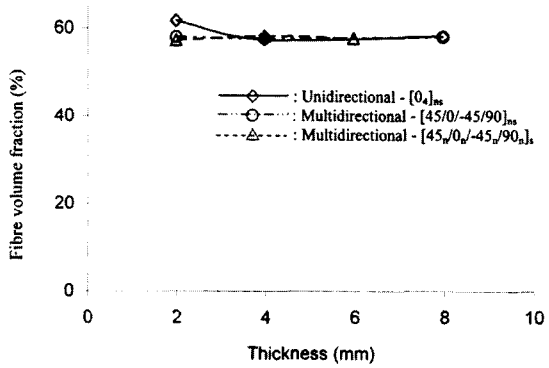

Fig. 9 Comparison of fibre volume fraction versus specimen thickness (unidirectional ($[0_4]_{ns}$) and multidirectional (sublaminate level scaling of $[45/0/-45/90]_{ns}$ and ply level scaling of $[45_n/0_n/-45_n/90_n]_s$) - T800/924C laminates)

fibre density) are required. Three specimens were tested from each test sample and the results were averaged.

Fig. 9 shows the average fibre volume fraction of unidirectional ($[0_4]_{ns}$) and multidirectional (sublaminate level scaling - $[45/0/-45/90]_{ns}$ and ply level scaling - $[45_n/0_n/-45_n/90_n]_s$) specimens as a function for specimen thickness. In the present study, 2 mm, 4 mm, 6 and 8 mm thick unidirectional and multidirectional specimens were selected to measure the fibre volume fraction. It is noticed from the figure that the fibre volume fraction measured for the 8 mm thick unidirectional specimen drops by about 7 % when compared to 2 mm thick specimen. No such changes are observed in the sublaminate or ply level scaled specimens with increasing specimen thickness. The fibre volume fraction is independent of the specimen thickness.

3.4 Void Content

It is well known that the possibility of finding voids in a composite laminate increases with increasing laminate volume and the presence of voids greatly affect the apparent stiffness and strength of composite laminates. In addition, voids can also significantly reduce the shear strength of composite materials[16]. When the void content is high in the matrix, the stiffness of the matrix is reduced and stress concentrations exist. When voids are trapped at the fibre/matrix interface, a weak or debonded interface contributes to the reduction of composite strength properties. A few studies, however, have been performed to measure the voids with increasing material volume.

Fig. 10 shows the average void content of unidirectional ($[0_4]_{ns}$) and multidirectional (sublaminate level scaling -

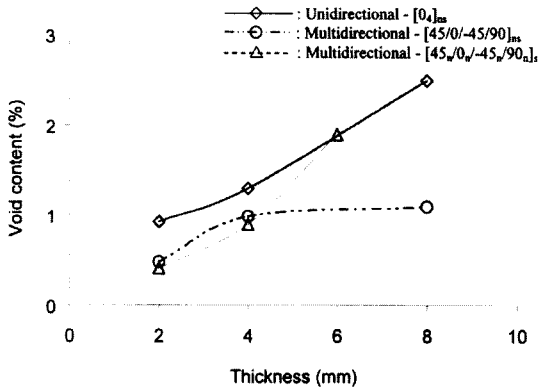

Fig. 10 Comparison of void content versus specimen thickness (unidirectional ($[0_4]_{ns}$) and multidirectional (sublaminate level scaling of $[45/0/-45/90]_{ns}$ and ply level scaling of $[45_n/0_n/-45_n/90_n]_s$).

$[45/0/-45/90]_{ns}$ and ply level scaling - $[45_n/0_n/-45_n/90_n]_s$) specimens versus specimen thickness. Unidirectional specimens 2 mm, 4 mm, and 8 mm thick were used to measure the void content. Void content as shown in Fig. 10 clearly increases with increasing specimen thickness. From the figure, it can be inferred that test data show an inverse relationship between void content and the respective strength. Bazhenov et *al*[17]. studied the effects of voids on the compression strength of a unidirectional composite. They found that the compression strength decreased with increasing void content. Like the unidirectional specimens, 2 mm, 4 mm and 8 mm thick multidirectional specimens fabricated with the sublaminate level scaling technique were used to measure the void content. It is shown that void content is dependent to the specimen thickness change but the increasing rate of void content for each thickness is not as high as the unidirectional ones. For 2 mm, 4 mm and 6 mm thick multidirectional specimen fabricated with the ply level scaling technique (blocked plies), the void content in the figure is rapidly increased with increasing specimen thickness. This trend is quite similar to the unidirectional specimens, indicating that the type of stacking sequence affects the laminate void content. Blocked lay-ups are expected to contain a higher number of defects resulting in bigger strength reductions

3.5 Fibre Waviness

Fibre waviness is a manufacturing defect caused by the manufacturing technique used such as filament winding, weaving, braiding, etc. Fibres are misaligned further during the curing process. Yugartis identified that the lamination process can change the fibre misalignment distribution or

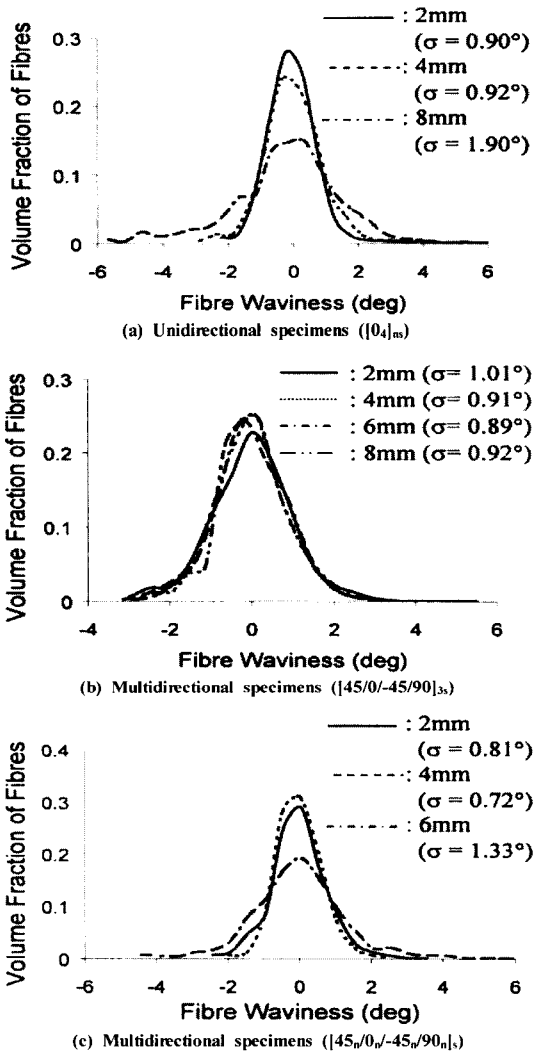

Fig. 11 Fibre waviness distribution for 2 mm, 4 mm, 6 mm and 8 mm thick unidirectional ($[0_4]_{ns}$) and multidirectional (sublaminate level scaling of $[45/0/-45/90]_{ns}$ and ply level scaling of $[45_n/0_n/-45_n/90_n]_s$) specimens.

different resin flow fields found in different composite systems could lead to changes in the distributions and ultimately differences in mechanical properties. The misalignment angle associated with fibre waviness has been reported to significantly influence longitudinal compressive strength[2,11,18,19].

In the present study, the extent of the fibre waviness was investigated according to the specimen thickness (2 mm, 4 mm, 6 mm and 8 mm) and compared with the standard deviation, σ, of the fibre angle distribution. The major axis

lengths of 1000 fibres for each sample were measured to calculate the in-plane fibre misalignment angle. Method and procedure to measure the waviness angle are explained in the references of 6 and 19.

Fig. 11 shows fibre waviness distribution as a function of specimen thickness (2 mm, 4 mm, 6 mm and 8 mm) and stacking sequence ($[0_4]_{ns}$, $[45/0/-45/90]_{ns}$ and $[45/0/-45/90]_{ns}$ In Fig. 11 (a), the comparison of fibre waviness distribution between unidirectional specimens with different thickness is presented. The distribution for the 8 mm thick specimen is clearly wider (σ = 1.90°) than those for 2 mm (σ = 0.90°) and 4 mm thick specimen (σ = 0.92°). The wider distribution means poor fibre alignment in the specimen.

Fig. 11 (b) shows that the distribution of the fibre waviness in the $[45/0/-45/90]_{ns}$ specimens is independent of specimen thickness but this is not the case for the blocked laminate $[45/0/-45/90]_{ns}$, Fig. 11 (c), where the fibre waviness distribution becomes wider corresponding to a bigger fibre misalignment. This may be caused by the movement of fibres during the curing process i.e. more likely to move due to the factors such as the fibre nesting and resin flow or resin release in the blocked 0° plies. Therefore, the compressive strength of the sublaminate level scaled specimens will not be affected by increasing specimen thickness since fibre waviness remains unchanged.

3.6 Free Edge Effects of Multidirectional Specimens

It is well known that interlaminar stresses develop at free edges in composite laminates because the individual anisotropic plies have different stiffness properties (E, G, ν). Free-edge delamination is mainly attributed to the existence of interlaminar stresses. In some laminates, it leads to premature failure initiating at the free edge, and the failure stress will then depend on the ply thickness[20]. For example, Lagace *et al.* and Kellas *et al*[21,22]. presented results that showed that each of the ply level scaled laminates exhibited a different tensile strength degradation with increasing laminate thickness. In conclusion, these authors have attributed the problem of strength degradation to interlaminar stress effects. Furthermore, Kim *et al*[23]. investigated numerically interlaminar stresses using sublaminate level scaled laminates ($[45/0/-45/90]_{ns}$) and ply level scaled laminates ($[45_n/0_n/-45_n/90_n]_s$) under tensile load. They reported that interlaminar stresses were mainly governed by stacking sequence but were also sensitive to thickness changes at the ply level.

In this section, the effect of laminate thickness and stacking sequence on interlaminar stresses in laminates under compressive load were investigated using finite element analysis (FE77)[12]. Sublaminate level scaled stacking sequence ([45/0/-45/90]ns) and ply level scaled stacking sequence ($[45_n/0_n/-45_n/90_n]_s$) were analysed for n = 2, 3, 4, 6 and 8., i.e. from 2 mm thick to 8 mm thick. A composite thick shell element (HS16) containing 8 nodes on the top surface and 8 nodes on the bottom surface is available in FE77. This element, like a conventional 3D finite element, has three degrees of freedom per node although, like a plate element, the strains are defined in the local directions of the mid-plane surface. The stress-strain property matrix of this element was modified to decouple the stresses in the local mid-plane and the strains normal to this plane thus preventing the element from being too stiff in bending[24]. A main advantage of this element is to improve the computational efficiency associated with the calculation.

Because of the symmetry of the problem, only a quarter of the laminate was analysed under uniform axial compressive load. One element per ply was used through the thickness. Refer to a representative finite element mesh model of a 4 mm thick specimen of reference 26.

From the results of the numerical analysis, maximum calculated σ_z values (through thickness normal stress) were found at 0/-45 ply interfaces of the first sublaminate for the sublaminate level scaled laminates, while the maximum σ_z values of the ply level scaled laminates are observed at 90/-45 ply interfaces. The maximum σ_z values of the sublmainate level scaled laminates are 11.9 %, 11.5 %, 12.7 %, 12.7 % and 12.6 % of the applied stress (σ^{∞}) for 2 mm, 3 mm, 4 mm, 6 mm and 8 mm thick laminates, respectively. The maximum σ_z values of the ply level scaled laminates are 26 %, 31.7 %, 31.7 %, 34.5 % and 37.4 % of the applied stress (σ^{∞}) for 2 mm, 3 mm, 4 mm, 6 mm and 8 mm thick laminates, respectively.

The peak values of interlaminar shear stress τ_{xz} for the sublaminate level scaled laminates were shown in the 0° plies of 2 mm and 3 mm thick laminates and at -45°/90° ply interfaces for 4 mm, 6 mm and 8 mm thick laminates. For the ply level scaled laminates, the peak interlaminar shear stresses τ_{xz} were found at 90°/45° ply interface for 2 mm and 3 mm thick laminates and 45°/0° ply interface for 4 mm, 6 mm and 8 mm thick laminates. The peak τ_{xz} values obtained for the ply level scaled laminate increase continuously from 4.7 % to 18 % of the applied stress (σ^{∞}) with increasing laminate thickness like the interlaminar normal

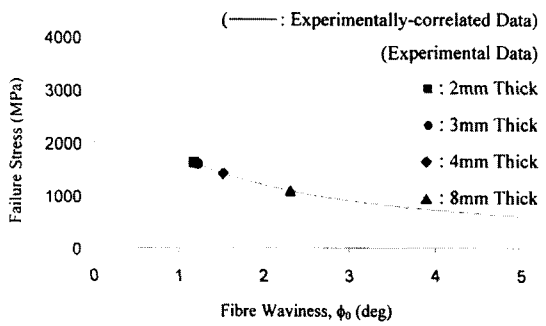

Fig. 12 Variation of longitudinal compressive strength with initial fibre waviness for the unidirectional composite laminate.

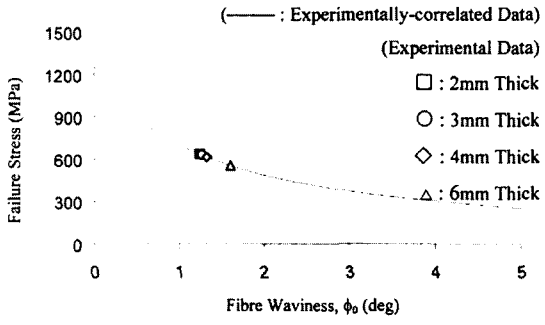

Fig. 13 Variation of predicted longitudinal compressive strength with initial fibre waviness for the multidirectional composite laminate ($[45_n/0_n/-45_n/90_n]_s$).

stresses, while the values from the sublaminate level scaled laminates are nearly constant regardless of the thickness change. It is found that the free edge interlaminar shear stress τ_{xz} is also sensitive to the stacking sequence like the interlaminar normal stress. These interlaminar normal and shear stresses can lead to edge delamination that under uniaxial compressive load may reduce the lateral support of the 0° plies triggering fibre microbuckling and premature laminate failure.

4. Prediction of Strength

The most frequently considered compressive failure modes in unidirectional laminates are fibre microbuckling and fibre kinking. On this basis, theoretical models analyse compressive failure using two major models, namely, the microbuckling model and the kink model. In the present study the fibre kink model (Budiansky model) for compressive strength prediction based on the assumed initial fibre waviness and the in-plane shear characteristics of the composite was adopted. The predicted compressive strength is matrix dominated and intimately related to the in-plane shear stress-strain behaviour of the lamina and the initial fibre waviness[18].

The experimentally - correlated compressive strengths are compared with the measured experimental values in Fig. 12. The measured 2 mm thick compressive strength of 1625 MPa corresponds to an initial fibre waviness of $\phi_0 \cong 1.17°$, which is similar to that determined by the graphical method (1.15°) described by Bardorf and Ko[19]. For the 8 mm thick specimens, the measured compressive strength of 1087 MPa is in accord with an initial fibre waviness of $\phi_0 \cong 2.31°$. The average fibre misalignment measured in accordance with Yurgartis method varied from 0.90° to 1.90° with increasing specimen thickness (2 mm to 8 mm thick), Fig. 11 (a).

For the T800/924C unnotched multidirectional laminates the compressive strength were predicted by using equation together with the maximum stress failure criterion. Fig. 13 shows the obtained failure strength as a function of initial fibre waviness and compared to the measured values of the ply level scaled specimens ($[45_n/0_n/-45_n/90_n]_s$). The measured compressive strength for the 2 mm and 6 mm thick specimens of 634 MPa and 553 MPa corresponds to an initial fibre waviness of $\phi_0 \cong 1.24°$ and 1.6°, respectively [19,20]. The fibre waviness angles measured by Yurgartis method were 0.81° for 2 mm and 1.33° for the 6 mm thick specimen. The failure strengths of the sublaminate level scaled specimens ($[45/0/-45/90]_{ns}$) are not presented in Fig. 13 since the specimens did not exhibit any thickness effect on the measured strengths (see Fig. 5).

5. Conclusion

In order to show the thickness effect on the compressive strength of composite laminates extensive static compressive tests were performed on unidirectional and multidirectional laminates 2 mm to 8 mm thick. In addition, parameters such as fibre volume fraction, void content, fibre waviness and interlaminar stresses, which influence the compressive failure strength, were investigated experimentally and numerically. Residual thermal stresses may also have an effect on strength especially of thick specimens but this was not investigated in the present study.

A thickness effect existed in the unidirectional specimens ($[0_4]_{ns}$) and the ply level scaled multidirectional specimens ($[45_n/0_n/-45_n/90_n]_s$). It was found that the main parameters introducing the thickness effect on the compressive failure strength are fibre waviness and void content. It was also

identified that fibre waviness is sensitive to the stacking sequence of the laminate and it increases with increasing thickness of the ply level scaled laminate. The compressive strength of the sublaminate level scaled specimens ($[45/0/-45/90]_{ns}$) was constant regardless of the specimen thickness (ply thickness remains constant) and the parameters (fibre volume fraction, void content, fibre waviness and interlaminar stresses) were quite independent of the specimen thickness. No thickness effect was observed in this type of stacking sequence.

References

1) Camponeschi, E. T., "Compression Testing of Thick-Section Composite Materials," *Composite Materials: Fatigue and Fracture (Third Volume), ASTM STP 1110, American Society for Testing and Materials*, Philadelphia, 1991, pp. 439-456.
2) Daniel, I. M. and Hsiao, H. M., "Is There a Thickness Effect on Compressive Strength of Unnotched Composite Laminates?," *International Journal of Fracture*, Vol. 95 (Special Issue), 1999, pp. 143-158.
3) Hsiao, H. M., Daniel, I. M. and Wooh, S. C., "A New Compression Test Methods for Thick Composites," *Journal of Composite Materials*, Vol. 29, No. 13, 1995, pp. 1789-1806.
4) Garala, H. J., "Experimental Evaluation of Graphite/Epoxy Composite Cylinders Subjected to External Hydrostatic Compressive Loading," *Proceedings*, 1987 Spring Conference on Experimental Mechanics, *Society for Experimental Mechanics*, Bethel, CT, 1987, pp. 948-951.
5) Bazant, P. Z., Kim, J. H., Daniel, I. M., Emilie, B. G. and Zi, G., "Size Effect on Compression Strength of Fibre Composites Failing By Kink Band Propagation," *International Journal of Fracture*, Vol. 95 (Special Issue), 1999, pp. 103-141.
6) Soutis, C. "Compressive Failure of Notched Carbon Fibre-Epoxy Panels," PhD thesis, *University of Cambridge*, UK, 1989.
7) Aribus Industrie Test Method, AITM-1008, Issue 2, June 1994.
8) Haberle, J. G., "Strength and Failure Mechanics of Unidirectional Carbon fibre-Reinforced Plastics under Axial Compression," PhD thesis, *University of London*, UK 1991.
9) Soutis, C., Lee, J. and Kong, C., "Size Effect on Compressive Strength of T300/924C Carbon Fibre-Epoxy Laminates," *Plastics, Rubber and Composites*, Vol. 3, No. 8, 2002, pp. 364-370
10) Flaggs, L. D. and Kural, H. M., "Experimental Determination of the In Situ Transverse Lamina Strength in Graphite/Epoxy Laminates," *Journal of Composite Materials*, Vol. 16 (March), 1982, pp. 103-116
11) Yugartis, S. W., "Measurement of Small Angle Fibre Misalignments in Continuous Fibre Composites," *Composite Science and Technology*, Vol. 30, No. 4, 1987, pp. 279-293.
12) Hitchings, D., "FE77 Users' Manual," Imperial College, Department of Aeronautics, 1995.
13) Kim, C. and White, S. R., "The Continuous Curing Process for Thermoset Polymer Composites. Part 2: Experimental Results for a Graphite/Epoxy Laminate," *Journal of Composite Materials*, Vol. 30, No. 5, 1996, pp. 627-647.
14) Chim, E. S. and Lo, K. H., "Compressive Strength of Unidirectional Composites," *Journal of Reinforced Plastics and Composites*, Vol. 11, 1992, pp. 838-896.
15) British Aerospace Test Methods, "Test Methods for the Fibre And void Content of Cured Carbon And Glass Fibre Composites," *BAER 3014*, ISSUE 3, 1990
16) McKenna, G. B., "Interlaminar Effects in Fibre-Reinforced Plastics ? A Review", *Polymer-Plastics Tech. Engin.*, Vol. 5, No. 1, 1975, pp. 23-53.
17) Bazhenov, S. L., Kuperman, A. M., Zelenskii, E. S. and Berlin, A. A., "Compression Failure of Unidirectional Glass-Fibre-Reinforced Plastics," *Composite Science and Technology*, Vol. 45, No. 3, 1992, pp. 201-208.
18) Budiansky, B. "Micromechanics," *Computers and Structures*, Vol. 16, No. 1-4, 1983, pp. 3-12.
19) Soutis, C., "Compressive Behaviour of Composites," *Rapra Review Reports*, Report 94, Vol. 8, No. 10, 1997.
20) Wisnom, M. R., "Size Effects in The Testing of Fibre-Composite Materials," *Composite Science and Technology*, Vol. 59, No. 13, 1999, pp. 1937-1957.
21) Lagace, P., Brewer, J., and Kassapoglou, C., "The Effect of Thickness of Interlaminar Stresses and Delamination in Straight-Edged Laminates," *Journal of Composites Technology & Research*, Vol. 9, No. 3, 1987, pp. 81-87.
22) Kellas, S. and Morton, J., "Strength Scaling in Fibre Composites," *AIAA Journal*, Vol. 30, No. 4, 1992, pp. 1074-1080.
23) Kim, J. K. and Hong, C. S., "Three-Dimensional Finite Element Analysis of Interlaminar Stresses in Thick

Composite Laminates," *Computers & Structures*, Vol. 40, No. 6, 1991, pp. 1395-1404.

24) Falzon, B. G., Hitchings, D. and Besant, T., "Fracture Mechanics Using a 3D Composite Element," *Composite Structures*, Vol. 45, No. 1, 1999, pp. 29-39.

25) Robert, M. J., "Mechanics of composite Materials," 2nd edition, *Taylor & Francis*, 1996, pp. 227-330.

26) Lee, J. "Compressive Behaviour of Composite Laminates Before and After Low Velocity Impact", PhD thesis, *Imperial College London*, UK, 2003.